

## Structural Transformation in Nb<sub>2</sub>O<sub>5</sub>-Promoted Rh Catalysts during Calcination and Reduction Treatments

Z. HU, H. NAKAMURA, K. KUNIMORI,<sup>1</sup> Y. YOKOYAMA,<sup>2</sup> H. ASANO, M. SOMA,\*  
AND T. UCHIJIMA<sup>1</sup>

*Institute of Materials Science, University of Tsukuba, Tsukuba, Ibaraki 305, Japan, and \*National Institute for Environmental Studies, Tsukuba, Ibaraki 305, Japan*

Received November 30, 1988; revised March 1, 1989

The extent of Rh–Nb<sub>2</sub>O<sub>5</sub> interaction in the niobia-promoted Rh/SiO<sub>2</sub> catalyst depends on parameters such as calcination temperature. For the Nb<sub>2</sub>O<sub>5</sub>-promoted Rh/SiO<sub>2</sub> catalyst with the Nb/Rh atomic ratio of unity, no significant SMSI effects were observed after air calcination at 773 K. However, this catalyst exhibits significant SMSI behaviors after calcination at higher temperatures (973 and 1173 K). After high-temperature reduction at 773 K, the capacity of H<sub>2</sub> chemisorption typically diminished almost to zero and the catalytic activity for ethane hydrogenolysis was suppressed by ca. 3.5 orders of magnitude compared with that after low-temperature reduction at 373 K. X-ray diffraction showed that the RhNbO<sub>4</sub> compound was formed, with the amount increasing with increasing calcination temperature. After air calcination at 1173 K, the RhNbO<sub>4</sub> compound was formed almost exclusively on the SiO<sub>2</sub> surface. The RhNbO<sub>4</sub> compound was reduced to Rh and NbO<sub>2</sub> during HTR treatment at 773 K, accompanied by splitting of the large RhNbO<sub>4</sub> particle into a number of smaller Rh particles. The mechanism of Rh–Nb<sub>2</sub>O<sub>5</sub> interaction is discussed. It is proposed that the NbO<sub>2</sub> species formed during the HTR treatment block surface Rh atoms to induce strong Rh–Nb<sub>2</sub>O<sub>5</sub> interaction (SMSI). © 1989 Academic Press, Inc.

### INTRODUCTION

There has been much interest in the strong metal–support interaction (SMSI) as well as in the effect of oxide promoter in supported metal catalysts (1–6). The metal–oxide interaction modifies the catalytic properties of the metal significantly (7–11). Evidence for a strong metal–support interaction has been observed in TiO<sub>2</sub>-promoted Rh catalysts (12) and in Nb<sub>2</sub>O<sub>5</sub>-promoted Ni catalyst (13). Such oxide promoters have also been reported to modify substantially the catalytic properties of the metal (5–7). Kunimori *et al.* reported that a Nb<sub>2</sub>O<sub>5</sub>-promoted Rh/SiO<sub>2</sub> catalyst exhibited SMSI behavior in ethane hydrogenolysis reaction, the Rh–Nb<sub>2</sub>O<sub>5</sub> interaction being as strong as that in the Rh/Nb<sub>2</sub>O<sub>5</sub>

catalysts (14). The results show that metal–support and metal–oxide promoter interactions are quite similar.

Metal–oxide interaction was discovered many years ago, and the early literature has been reviewed by Solymosi and Schwab (15, 16). Tauster and co-workers first reported SMSI phenomena (17, 18). This work has led to numerous studies on the interesting properties of many transition metals supported on reducible oxides. The studies have enhanced our understanding of the mechanism of the strong metal–support interaction (19–29). In a current model of SMSI, a reduced oxide species is formed during high-temperature reduction (HTR) and then blocks surface metal atoms, leading to a suppression in the capacity of H<sub>2</sub> chemisorption and in the catalytic activity for ethane hydrogenolysis reaction (“decoration model”) (20, 30). However, the structure of the reduced oxide species and their interaction with metal still remain unclear.

<sup>1</sup> To whom correspondence should be addressed.

<sup>2</sup> Present address: Corporate Research and Development Laboratory, Toa Nenryo Kogyo K. K., Ohimachi, Iruma, Saitama 354, Japan.

The term "SMSI behavior" is used in this paper for the cases which meet the definition in the original observations (17, 18), i.e., a drastic suppression of chemisorption ability and/or catalytic activity after high-temperature reduction and its recovery after high-temperature  $O_2$  treatment followed by low-temperature reduction (LTR). SMSI behavior has been amply confirmed in the originally reported catalyst systems (metal/ $TiO_2$ , metal/ $Nb_2O_5$ , etc.), and new catalyst systems ( $TiO_2$ -,  $V_2O_5$ -, and  $Nb_2O_5$ -promoted metal catalysts) have been observed to exhibit equivalent behavior (4, 12, 13, 29). Because the amount of the reducible oxide is significantly smaller in the latter catalyst systems, we may be able to obtain clearer information about the structure of the oxide which interacts strongly with metal. For the promoted metal catalysts, mixed oxide may be formed between metal and oxide promoter. This chemistry will affect the degree of metal-oxide interaction. Formation of the  $RhVO_4$  mixed oxide has been proposed in  $V_2O_5$ -promoted Rh catalysts by Kip *et al.* (31). They found that vanadium oxide hampers the reduction of rhodium oxide in  $Rh/V_2O_5/SiO_2$  catalysts, which do not contain "free"  $V_2O_5$  when the ratio of V/Rh is 0.9. In the preceding papers (32, 33), we have found a formation of  $RhNbO_4$  as a new phase by X-ray diffraction during calcination of the  $Nb_2O_5$ -promoted  $Rh/SiO_2$  catalyst. It has also been suggested that the  $Nb_2O_5$  on the  $SiO_2$  surface migrates toward the rhodium particle during the calcination process to form the  $RhNbO_4$  compound. Such  $Nb_2O_5$  or  $RhNbO_4$  is reduced during high-temperature reduction, and spreads on the surface of Rh particles, leading to the suppression of  $H_2$  chemisorption capacity and ethane hydrogenolysis activity. Significant SMSI effects have been observed in the  $Nb_2O_5$ -promoted 0.5%  $Rh/SiO_2$  (Nb/Rh = 9.3) and  $Nb_2O_5$ -promoted 5%  $Rh/SiO_2$  (Nb/Rh = 3.1) catalysts (32). Because these catalysts contain an excess amount of  $Nb_2O_5$  promoter, a large part of which does not inter-

act directly with rhodium, little information about the structure of reduced niobia species and its interaction with Rh have been obtained so far. Thus, an attempt to use a  $Nb_2O_5$ -promoted  $Rh/SiO_2$  catalysts with the Nb/Rh atomic ratio of unity might help us to understand in detail the migration and reduction behavior of rhodium and niobia promoter on the silica surface.

In this paper, the results of our recent work using  $Nb_2O_5$ -promoted Rh catalysts (Nb/Rh = 1.0) and  $RhNbO_4/SiO_2$  catalysts as starting materials will be presented. TPR, TPO, and XPS experiments were carried out to characterize the Rh- $Nb_2O_5$  interaction. The structure change of the catalyst was studied by X-ray diffraction. The catalytic properties and the characterization results will be described first, followed by a discussion of the mechanism of Rh- $Nb_2O_5$  interaction and the structure of the reduced niobia species in the SMSI state.

## EXPERIMENTAL

*Preparation of catalyst.* A silica of Japan reference catalyst (JRC-SIO-3, BET surface area of  $186\text{ m}^2/\text{g}$ ) was used as support (34). After calcination in air at 773 K, the  $SiO_2$  support was impregnated with a mixed aqueous solution of  $RhCl_3$  and  $(NH_4)_3[NbO(C_2O_4)_3]$ , and then dried at 393 K overnight. Catalysts A and B were obtained by calcining this impregnated sample in air at 773 K for 1 h and at 973 K for 3 h. Rhodium content was 4.8 wt%. For catalyst C, the  $SiO_2$  support was precalcined in air at 1173 K for 3 h, to avoid possible structural change during the following high-temperature calcination. The BET surface area decreased to  $40\text{ m}^2/\text{g}$ . A 4.2 wt%  $Rh/SiO_2$  catalyst was prepared by impregnation of the precalcined silica with a solution of  $RhCl_3$ , then dried at 393 K but not calcined. This sample was then impregnated with  $(NH_4)_3[NbO(C_2O_4)_3]$  dissolved in deionized water. Catalyst C was obtained by calcining this sample in air at 1173 K for 3 h after it had been dried at 393 K overnight. For all

the catalysts, the Nb<sub>2</sub>O<sub>5</sub> loading was chosen so that the atomic ratio of Nb/Rh is unity.

**H<sub>2</sub> chemisorption.** Volumetric H<sub>2</sub> chemisorption was measured in a conventional glass vacuum system, as described in (35). The catalyst was pretreated in O<sub>2</sub> at 773 K for 1 h, followed by low-temperature reduction at 373 K or high-temperature reduction at 773 K in H<sub>2</sub> flow purified with a liquid nitrogen trap. Before the measurement of H<sub>2</sub> adsorption at room temperature, the catalyst was evacuated at the catalyst reduction temperature for 1 h.

**O<sub>2</sub> consumption.** The O<sub>2</sub> consumption was studied in the same glass vacuum system. After the measurement of H<sub>2</sub> adsorption, the catalyst was evacuated at 773 K for 1 h to remove possible H<sub>2</sub> adsorbate on the catalyst. After the admission of O<sub>2</sub>, the catalyst was heated at 773 or 873 K. The O<sub>2</sub> uptake was instantaneous; it was followed by a gradual change, the rate of which became negligible after 1–2 h. Therefore, the amount of O<sub>2</sub> consumption was measured after being heated at 773 for 3 h or at 873 K for 1.5 h.

**Ethane hydrogenolysis.** The catalytic activity measurements for the ethane hydrogenolysis reaction were performed in a microcatalytic pulse reactor (36). The details of the procedure have been described elsewhere (32). The reaction was carried out after the catalyst was pretreated in O<sub>2</sub> at 673 K, followed by low-temperature reduction at 373 K or high-temperature reduction at 773 K.

**X-ray diffraction (XRD).** The XRD measurements were performed with an X-ray diffractometer (Rigaku Co. Ltd.) with a graphite monochromator for CuK $\alpha$  (40 kV, 30 mA) radiation. An on-line computer was used for data collection and processing, which made available the precise determination of *d* spacing values of diffraction lines. For normal measurements (continuous scan), slower scan speed (0.5°/min) was used. For step scan measurements, a scan step of 0.04° and a preset time of 20 s were employed.

**X-ray photoelectron spectroscopy (XPS).** XPS spectra were obtained using a VG ESCA LAB-5 spectrometer equipped with both AlK $\alpha$  and MgK $\alpha$  X-ray sources, a preparation chamber, and signal averager (35). The signal of Si 2*p* at 103.3 eV was used as a standard for the evaluation of core-electron binding energies.

**Temperature-programmed reduction (TPR).** The TPR measurements were performed in a flow system with the catalyst (0.25 g) placed in a microreactor connected to a quadrupole mass spectrometer, as described previously (32). After the catalyst was calcined in O<sub>2</sub> flow at 773 K for 1 h, it was purged with He gas at 773 K to remove any possible oxygen adsorbate over the support. The catalyst was subsequently cooled in He to room temperature; then a mixture of 1.04% H<sub>2</sub>-He was passed through the catalyst bed at 30 cm<sup>3</sup>/min, and the H<sub>2</sub> consumption was monitored as the catalyst temperature was raised at 5 K/min up to 973 K.

**Temperature-programmed oxidation (TPO).** TPO measurements were carried out in the same flow system. After the catalyst (0.25 g) was reduced at the desired temperature, it was purged with He purified at liquid nitrogen temperature by raising the temperature to 973 K to remove H<sub>2</sub> adsorbate on the catalyst. The sample was subsequently cooled in He to room temperature; then a mixture of 0.105% O<sub>2</sub>-He was passed through the catalyst bed at 30 cm<sup>3</sup>/min, and the O<sub>2</sub> consumption was monitored as the catalyst temperature was raised at 10 K/min to 973 K.

## RESULTS

The catalytic properties of the Nb<sub>2</sub>O<sub>5</sub>-promoted Rh catalysts are presented in Table 1. The fresh catalyst was first reduced in H<sub>2</sub> at 773 K (HTR) before any adsorption or activity measurements. As will be presented later, this first HTR treatment was performed to decompose the RhNbO<sub>4</sub> compound. It can thus be considered that the obtained chemisorption capacities and ac-

TABLE I  
Catalytic Properties of Nb<sub>2</sub>O<sub>5</sub>-Promoted Rh/SiO<sub>2</sub>  
Catalysts

Catalyst	H/Rh <sup>a</sup>		Extent of activity suppression <sup>b</sup>	Rh particles <sup>c</sup>	
	LTR	HTR		Mean size (Å)	Dispersion
Catalyst A	0.061	0.020	1	43	0.21
Catalyst B	0.053	0.003	10 <sup>-3.5</sup>	85	0.11
Catalyst C	0.130	0.004	10 <sup>-3.5</sup>	48	0.19

<sup>a</sup> The fresh catalyst was first reduced in H<sub>2</sub> at 773 K (1st HTR) before the chemisorption and activity measurements. Chemisorption capacities were measured after high-temperature reduction at 773 K (HTR) and O<sub>2</sub> treatment at 773 K followed by low-temperature reduction at 373 K (LTR).

<sup>b</sup> The extent of activity suppression is given as a ratio of the catalytic activity for ethane hydrogenolysis after HTR treatment at 773 K to that after LTR treatment at 373 K ( $r_{\text{HTR}}/r_{\text{LTR}}$ ).

<sup>c</sup> The mean size and dispersion of Rh particles were obtained from X-ray diffraction of the catalyst reduced in H<sub>2</sub> at 773 K according to the Scherrer formula.

tivities are the catalytic properties of the Rh particles. For catalyst A (calcined at 773 K), almost the same catalytic activities were observed after LTR at 373 K and HTR at 773 K. However, significant suppression effects were observed in catalysts B and C, which were calcined in air at higher temperatures (973 and 1173 K, respectively). After the O<sub>2</sub> treatment followed by LTR, the catalytic activity of catalyst B increased by ca. 3.5 orders of magnitude relative to that after the first HTR treatment. For catalyst C, the observed suppression extent was almost the same as that in catalyst B. The suppression was reversible. Following the first HTR treatment, the catalytic activity of catalyst C increased (by ca. 3.2 orders of magnitude) after the O<sub>2</sub> treatment at 673 K followed by LTR treatment. This activity decreased (by ca. 3.5 orders) again after the following HTR treatment. Almost the same suppression extents were observed after the first and second HTR treatments (39).

The results of H<sub>2</sub> chemisorption and XRD studies are also shown in Table I. The H/Rh values from H<sub>2</sub> chemisorption measurements are less than those Rh dispersions obtained by X-ray diffraction. This result suggests that the Rh particles are partially covered with the Nb<sub>2</sub>O<sub>5</sub> promoter

even after LTR, as reported previously (32). The mean size of Rh particles is different for the Nb<sub>2</sub>O<sub>5</sub>-promoted Rh catalysts calcined at different temperatures. The size is 43 Å for catalyst A. This size increased to 85 Å after the catalyst was calcined at higher temperature (catalyst B). However, the particle size decreased to 48 Å in catalyst C, even though the catalyst was calcined at much higher temperature (1173 K). It is interesting that the mean size of Rh particles of catalyst C is smaller than that of catalyst B.

The H<sub>2</sub> chemisorption capacity decreased with increasing catalyst reduction temperature. In catalyst A, substantial H<sub>2</sub> chemisorption (about one-third of the value after LTR at 373 K) was observed even after HTR at 773 K. However, the capacity of H<sub>2</sub> chemisorption diminished almost to zero in catalysts B and C. Apparently, the Nb<sub>2</sub>O<sub>5</sub>-promoted Rh catalysts more or less show the behaviors characteristic of SMSI phenomena in H<sub>2</sub> chemisorption and ethane hydrogenolysis reaction, because both the chemisorption capacities and the catalytic activities decrease with increasing catalyst reduction temperature. As suggested by the decoration model of SMSI, the suppression effects are due to the blockage of surface Rh atoms. It thus can be considered that in catalyst A only part of the Rh interacts with the niobia promoter, but almost all of the surface Rh atoms are blocked by the niobia promoter in catalysts B and C after HTR. The different extent of SMSI in catalysts A and B supports our previous conclusion that the extent of Rh–Nb<sub>2</sub>O<sub>5</sub> interaction is increased by calcining the Nb<sub>2</sub>O<sub>5</sub>-promoted Rh catalyst in air at higher temperature (32).

In order to characterize the structure of rhodium and niobia promoter, X-ray diffraction patterns were recorded after the catalysts were treated in H<sub>2</sub> or O<sub>2</sub> at different temperatures. For catalyst A, which was calcined in air at 773 K, only a few broad diffraction peaks were observed, which can be attributed to Rh<sub>2</sub>O<sub>3</sub> (Fig. 1,

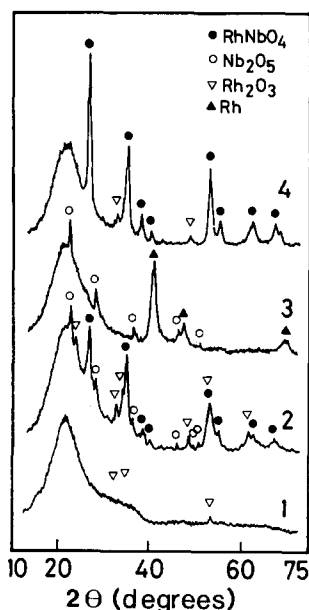


FIG. 1. X-ray diffraction patterns of Nb<sub>2</sub>O<sub>5</sub>-promoted Rh catalysts calcined at different temperatures. (1) Catalyst A (calcined in air at 773 K). (2) Catalyst B (calcined in air at 973 K). (3) Catalyst B after being reduced in H<sub>2</sub> at 773 K. (4) Catalyst B after being calcined in air at 1173 K.

No. 1). It suggests that Nb<sub>2</sub>O<sub>5</sub> is dispersed well or amorphously. However, the diffraction pattern of catalyst B calcined at 973 K is more complex. As shown in Fig. 1 (No. 2), three phases (Rh<sub>2</sub>O<sub>3</sub>, Nb<sub>2</sub>O<sub>5</sub>, and RhNbO<sub>4</sub>) are observed. A new phase of RhNbO<sub>4</sub> compound was formed between Rh and Nb<sub>2</sub>O<sub>5</sub> promoter. The XRD pattern of catalyst B after H<sub>2</sub> reduction at 773 K is also presented in Fig. 1 (No. 3). The diffraction peaks of the Rh metal are observed with the disappearance of the RhNbO<sub>4</sub> phase. However, it should be noted that no reduction was observed in the intensities of the diffraction peaks of the Nb<sub>2</sub>O<sub>5</sub> phase (Nos. 2 and 3).

Catalyst B was further calcined at a higher temperature (1173 K). The XRD pattern is shown in Fig. 1, No. 4. The intensities of the diffraction peaks of the RhNbO<sub>4</sub> compound increased substantially. At the same time, the diffraction peaks of the Nb<sub>2</sub>O<sub>5</sub> phase disappeared in the XRD pat-

tern (No. 4), implying that a reaction occurred between rhodium and the niobia promoter:



The Rietveld analysis of X-ray powder diffraction data was carried out in order to reconfirm the previous assignment (32). Figure 2 illustrates the profile fit and the difference patterns for catalyst B after calcination at 1173 K. Crosses are observed intensities, the solid line overlying them is the calculated intensity, and  $\Delta y_i$  is the difference between observed and calculated intensities. The short vertical lines mark the positions of possible Bragg peaks of the RhNbO<sub>4</sub> compound. The observed XRD pattern contains the RhNbO<sub>4</sub> compound almost exclusively with a little of the Rh<sub>2</sub>O<sub>3</sub> phase. Figure 2 shows that the calculated pattern fits the observed one well. The tetragonal lattice parameters of the RhNbO<sub>4</sub> compound were refined to be  $a = 4.708 \text{ \AA}$ ,  $c = 3.017 \text{ \AA}$ . This result is also in reasonable agreement with those of RhNbO<sub>4</sub> powders ( $a = 4.685 \text{ \AA}$ ,  $c = 2.980 \text{ \AA}$ ) by Shaplygin *et al.* (37).

In catalyst C, the silica support precalcined at 1173 K was used and calcined finally at the same temperature after its preparation. The XRD patterns of catalyst C are shown in Fig. 3 (No. 1). All the diffraction peaks correspond to the RhNbO<sub>4</sub> phase, except for a small peak due to the Rh<sub>2</sub>O<sub>3</sub> phase. No peaks corresponding to the Nb<sub>2</sub>O<sub>5</sub> oxide are observed. The pattern is in good agreement with that of catalyst B calcined at 1173 K (Fig. 1, No. 4). Therefore, the RhNbO<sub>4</sub> compound has been formed almost exclusively on the SiO<sub>2</sub> surface by the high-temperature calcination at 1173 K. After the H<sub>2</sub> reduction at 473 K, the small Rh<sub>2</sub>O<sub>3</sub> peak disappeared with the appearance of a small Rh metal peak (No. 2).

The structure changes of the RhNbO<sub>4</sub> phase are presented by XRD patterns in Fig. 4 after H<sub>2</sub> or O<sub>2</sub> treatments. Curve 1 is the XRD pattern of catalyst C after H<sub>2</sub> reduction at 773 K, where the diffraction

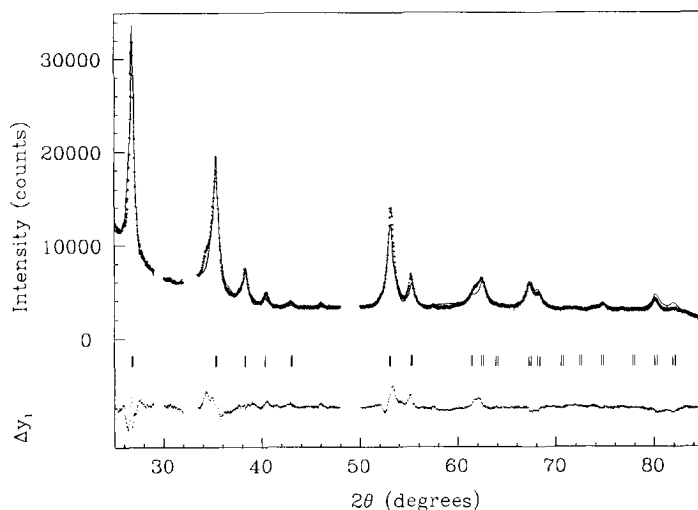


FIG. 2. Rietveld refinement patterns for the  $\text{RhNbO}_4$  compound in catalyst B after being calcined at 1173 K.

peaks of the  $\text{RhNbO}_4$  phase disappeared, and only the main diffraction peak (111) of the Rh metal appeared, but almost no other peaks of the Rh phase were observed. A small peak around  $26.0^\circ$  was observed, and its  $d$  spacing value ( $3.421 \text{ \AA}$ ) is the same as that of the most intensive diffraction line (400) of the  $\text{NbO}_2$  phase ( $3.42 \text{ \AA}$ ). This diffraction peak can be distinguished signifi-

cantly from the most intensive (110) peak of  $\text{RhNbO}_4$  ( $3.321 \text{ \AA}$ ) or other phases such as  $\text{Nb}_2\text{O}_5$ ,  $\text{Rh}_2\text{O}_3$ , etc. After catalyst C was

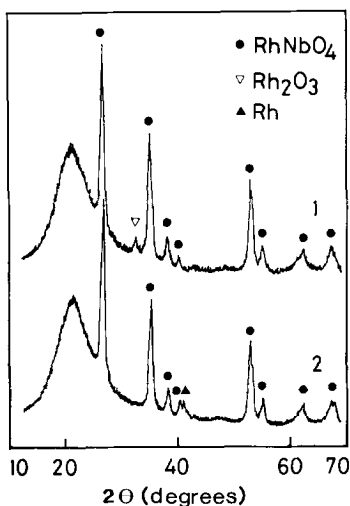


FIG. 3. X-ray diffraction patterns of catalyst C. (1) Catalyst C (calcined in air at 1173 K). (2) After step 1, the catalyst was reduced in  $\text{H}_2$  at 473 K.

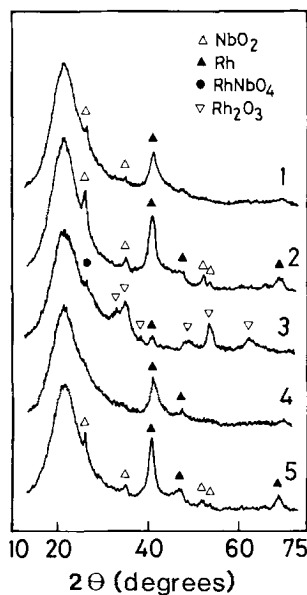


FIG. 4. X-ray diffraction patterns of catalyst C after being treated in  $\text{H}_2$  or  $\text{O}_2$ . (1) Catalyst C reduced in  $\text{H}_2$  at 773 K. (2) After step 1, the catalyst was treated in He at 973 K. (3) After step 1, the catalyst was calcined in air at 773 K. (4) After step 3, the catalyst was reduced in  $\text{H}_2$  at 773 K. (5) After step 4, the catalyst was treated in He at 973 K.

calcined in He at 973 K following reduction at 773 K, the diffraction pattern of this phase became more clear (No. 2). A best-fit was obtained if we calculate the  $d$  spacing values by assuming the tetragonal NbO<sub>2</sub> structure ( $a = 13.71$  Å,  $c = 5.985$  Å). We can thus conclude that the RhNbO<sub>4</sub> compound is reduced to the Rh metal, accompanied with the formation of reduced niobia species (NbO<sub>2</sub>).

O<sub>2</sub> treatment at 773 K has always been used to restore the normal state from SMSI. The XRD pattern after calcination in air at 773 K is shown in No. 3. The main peaks correspond to the Rh<sub>2</sub>O<sub>3</sub> phase. The diffraction peaks of the NbO<sub>2</sub> phase disappeared, probably as a consequence of oxidation to Nb<sub>2</sub>O<sub>5</sub>. A small diffraction peak of the Rh metal was still observed (No. 3). It indicates that the calcination treatment at 773 K is not sufficient to oxidize the Rh particles completely.

High-temperature reduction treatment can induce SMSI again after restoration by O<sub>2</sub> treatment. The XRD pattern after the HTR treatment at 773 K is shown in Fig. 4 (No. 4). Only the Rh phase was observed. The XRD pattern is similar to that after the first HTR treatment (No. 1), except for the absence of the NbO<sub>2</sub> diffraction peak at 26°. XRD pattern No. 5 was obtained after thermal treatment in He at 973 K following the second HTR treatment. The diffraction peaks of the Rh metal became sharper, indicating some agglomeration of Rh particles during the He treatment at 973 K. The diffraction peaks of NbO<sub>2</sub> were also observed in pattern No. 5, although the intensity was less than that in pattern No. 2. It should be pointed out that no NbO<sub>2</sub> phase was observed even after the same He thermal treatment when the catalyst was reduced at 473 K. Therefore, it can be considered that He treatment at 973 K mainly caused the highly dispersed NbO<sub>2</sub> to agglomerate to large crystallines.

X-ray photoelectron spectroscopy was used to characterize the Rh catalysts in the oxidized state. The binding energies of Rh

$3d_{5/2}$  are presented in Table 2. For the non-promoted Rh/SiO<sub>2</sub> catalyst which was calcined in air at 973 K, the Rh  $3d_{5/2}$  binding energy is 308.1 eV. In catalyst C calcined at 1173 K, the Rh  $3d_{5/2}$  binding energy is 309.1 eV. From the results of X-ray diffraction, the main phase is Rh<sub>2</sub>O<sub>3</sub> in the nonpromoted Rh catalyst, and RhNbO<sub>4</sub> in catalyst C after these treatments. It can thus be concluded that the Rh  $3d_{5/2}$  binding energies are 308.1 eV for Rh<sub>2</sub>O<sub>3</sub> and 309.1 eV for RhNbO<sub>4</sub> particles on the SiO<sub>2</sub> surface. Therefore, the formation of mixed oxide with Nb<sub>2</sub>O<sub>5</sub> induces a shift in the Rh  $3d_{5/2}$  binding energies to the higher energy side. After the RhNbO<sub>4</sub> has been once reduced and then treated in O<sub>2</sub> at 773 K, the observed Rh  $3d_{5/2}$  binding energy is 308.2 eV, which coincides quite well with that in the Rh<sub>2</sub>O<sub>3</sub> phase. The results should be compared with the observation by X-ray diffraction which shows the coexistence of Rh<sub>2</sub>O<sub>3</sub> and Rh as the main phases. However, no Rh metal was detected by XPS. This difference between XRD and XPS leads to the interpretation that the O<sub>2</sub> treatment at 773 K causes the oxidation of the outer layer of the Rh particles to Rh<sub>2</sub>O<sub>3</sub>, with the Rh core still unchanged. For catalyst B, which was calcined in air at 973 K, the observed Rh  $3d_{5/2}$  binding energy is 308.9 eV, in reasonable agreement with that of the RhNbO<sub>4</sub> compound. However, the result of X-ray diffraction shows that the catalyst contains two kind of rhodium:

TABLE 2  
Binding Energies of Rh  $3d_{5/2}$  in Nb<sub>2</sub>O<sub>5</sub>-Promoted Rh Catalysts

Catalyst	Calcination temperature (K)	Binding energy of Rh $3d_{5/2}$ (eV)
Catalyst C	1173	309.1
Catalyst C <sup>a</sup>	773	308.2
Catalyst B	973	308.9
5 wt% Rh/SiO <sub>2</sub>	973	308.1

<sup>a</sup> After catalyst C had been reduced in H<sub>2</sub> at 773 K, it was calcined in O<sub>2</sub> at 773 K.

$\text{Rh}_2\text{O}_3$  and  $\text{RhNbO}_4$ . No significant contribution of  $\text{Rh}_2\text{O}_3$  was observed by XPS. This can lead to the interpretation that calcination results in the formation of the  $\text{RhNbO}_4$  compound on the surface layer of  $\text{Rh}_2\text{O}_3$  particles.

Temperature-programmed reduction was used to study the interaction between rhodium and the niobia promoter in the oxide state. Figure 5 shows the TPR spectra of catalyst C. By calcination in air at 1173 K, the reduction peak shifted significantly to the higher temperature side (Fig. 5, No. 1), considering that the observed reduction temperature of  $\text{Rh}_2\text{O}_3$  was about 350 K for the nonpromoted  $\text{Rh}/\text{SiO}_2$  catalysts (32). The  $\text{H}_2$  consumption has a maximum around 800 K. A small reduction peak around 440 K was also observed at the lower temperature side. The calcination of the catalyst in  $\text{O}_2$  at 773 K after  $\text{H}_2$  reduction at 773 K gives the TPR profile No. 2 shown in Fig. 5.  $\text{H}_2$  consumption is observed mainly around 350–580 K, with a broad tail up to 870 K. As also discussed in a previous paper (32), the reduction peak at higher temperatures (about 800 K) can be attributed to the crystallized  $\text{RhNbO}_4$  compound (No. 1). Thus, the  $\text{H}_2$  consumption at the tailing part to 873 K in profile No. 2 may correspond to the reduction of the  $\text{RhNbO}_4$  precursor (surface compound) (32). The  $\text{H}_2$  consumption at the lower temperature side is due to the reduction of  $\text{Rh}_2\text{O}_3$  oxide, although its reduction temperature could have shifted to higher temperatures by interaction with the  $\text{Nb}_2\text{O}_5$  pro-

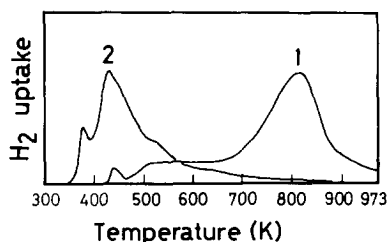


FIG. 5. TPR spectra of catalyst C. (1) Catalyst C calcined in air at 1173 K. (2) Following the  $\text{H}_2$  reduction at 773 K, catalyst C was calcined in  $\text{O}_2$  at 773 K.

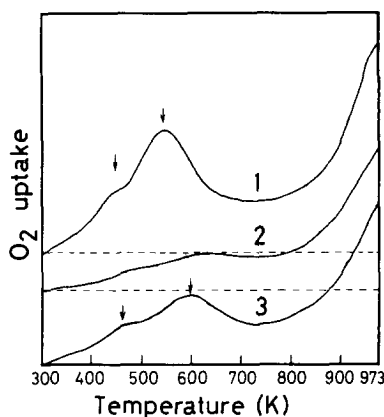


FIG. 6. TPO spectra of catalyst C. (1) Catalyst C after being reduced in  $\text{H}_2$  at 773 K. (2) Following  $\text{H}_2$  reduction at 773 K, catalyst C was calcined in  $\text{O}_2$  at 773 K and reduced in  $\text{H}_2$  at 473 K. (3) Following  $\text{H}_2$  reduction at 773 K, catalyst C was calcined in  $\text{O}_2$  at 773 K and reduced again in  $\text{H}_2$  at 773 K.

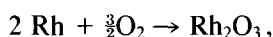
moter. The XRD results also support such interpretations, in which the main phase is assigned to  $\text{RhNbO}_4$  in TPR profile No. 1, and to  $\text{Rh}_2\text{O}_3$  in TPR profile No. 2.

In order to obtain more information about the structure of the reduced niobia species, temperature-programmed oxidation spectra were measured. The TPO profile of catalyst C ( $\text{RhNbO}_4/\text{SiO}_2$ ) after reduction at 773 K is presented in Fig. 6 (No. 1). The  $\text{O}_2$  consumption has a maximum around 540 K and another maximum at temperatures higher than 973 K. Because of the large Rh particle size of the catalyst and the low  $\text{O}_2$  concentration (0.105%  $\text{O}_2$ ) used in TPO measurements, higher temperatures are needed for complete oxidation. The  $\text{O}_2$  consumption peak at the higher temperature side can be considered the oxidation of the bulk Rh metal. The  $\text{RhNbO}_4$  compound was reduced in  $\text{H}_2$  at 773 K and then calcined in  $\text{O}_2$  at 773 K. The TPO profile No. 2 is observed as shown in Fig. 6, after the  $\text{H}_2$  reduction at 473 K for this catalyst. The  $\text{O}_2$  consumption peak at the higher temperature side remained almost unchanged, but the amount of  $\text{O}_2$  consumption at the lower temperature side decreased substantially. In Fig. 6 (No. 3), the TPO



profile is presented after the second HTR treatment at 773 K. The O<sub>2</sub> consumption increased at the lower temperature side, compared with No. 2. In contrast to the first HTR (Fig. 6, No. 1), however, a significant decrease was observed in the amount of O<sub>2</sub> consumption at the lower temperature side. As will be discussed later, the oxidation peak at the lower temperature side can be attributed to the oxidation of the reduced niobia species.

O<sub>2</sub> consumption was studied by a static vacuum system to estimate the amount of reduced niobia species. For the complete oxidation of Rh metal,



the amount of O<sub>2</sub> consumption is 1.5 in O/Rh value. For the Nb<sub>2</sub>O<sub>5</sub>-promoted Rh/SiO<sub>2</sub> catalysts evacuated at high temperature (773 K) after reduction, oxygen is consumed mainly for the oxidation of Rh metal and reduced niobia species. The part of O<sub>2</sub> consumption exceeding 1.5 in O/Rh value should be attributed to the oxidation of reduced niobia species.

The results are presented in O/Rh values in Table 3. In the second column are shown

the values of O<sub>2</sub> consumption after the H<sub>2</sub> reduction at 473 K for the catalyst which experienced first HTR followed by oxidation at 773 or 873 K. For catalyst A, the amount of O<sub>2</sub> consumption is 1.45 in O/Rh value after H<sub>2</sub> reduction at 473 K. This value is in reasonable agreement with that for complete oxidation of the Rh metal. In catalyst C, the amount of O<sub>2</sub> consumed during the thermal treatment at 773 K is 1.12 in O/Rh value after H<sub>2</sub> reduction at 473 K. When the thermal treatment was carried out in O<sub>2</sub> at 873 K, the observed O<sub>2</sub> consumption increased to 1.42 in O/Rh value. The above results suggest that the thermal treatment at 773 K is sufficient to oxidize Rh particles in catalyst A, but a higher temperature (873 K) is needed for catalyst C.

After the first HTR treatment at 773 K, the amount of O<sub>2</sub> consumed by catalyst A is 1.60 in O/Rh value. It implies that some reduced niobia species have been formed with the amount of about 0.1 in O/Rh value. Almost the same O<sub>2</sub> consumption was observed after the first and the second HTR treatment at 773 K in catalyst A.

For catalyst C, the data for both thermal treatments at 773 and 873 K are presented in Table 3 for comparison. In all cases, the O<sub>2</sub> consumption values during thermal treatment at 773 K are less than those at 873 K. As discussed above, it is more appropriate to estimate the amount of reduced niobia species from the data at 873 K. The amount of O<sub>2</sub> consumption is 2.02 in O/Rh value after the first HTR at 773 K. This value is significantly higher than those of any of the successive reduction treatments. The result indicates that some irreversible change occurred in catalyst C. Following the first HTR at 773 K, the O<sub>2</sub> consumption is 1.42 after H<sub>2</sub> reduction at 473 K. This value increased to 1.66 after the second HTR at 773 K. The O<sub>2</sub> consumption increased with increasing catalyst reduction temperature, implying that more Nb<sub>2</sub>O<sub>5</sub> promoter was reduced by H<sub>2</sub> reduction at a higher temperature. The amount of reduced niobia species was about 0.52 in O/Rh value

TABLE 3

Amount of O<sub>2</sub> Consumption for Nb<sub>2</sub>O<sub>5</sub>-Promoted Rh Catalyst

Catalyst	O <sub>2</sub> consumption (O/Rh) <sup>a</sup> after H <sub>2</sub> treatments at varying temperatures			
	(1) 1st HTR	(2) 473 K	(3) 573 K	(4) 2nd HTR
Catalyst A <sup>b</sup>	1.60	1.45	—	1.59
Catalyst C <sup>c</sup>	2.02	1.42	1.50	1.66
Catalyst C <sup>b</sup>	1.91	1.12	1.31	1.56

<sup>a</sup> The O<sub>2</sub> consumption measurements were made according to the following sequence: (1) 1st HTR at 773 K, (2) H<sub>2</sub> reduction at 473 K, (3) H<sub>2</sub> reduction at 573 K, and (4) 2nd HTR at 773 K.

<sup>b</sup> The amount of O<sub>2</sub> consumed during thermal treatment at 773 K.

<sup>c</sup> The O<sub>2</sub> consumption during thermal treatment at 873 K.

after the first HTR at 773 K, but decreased to 0.16 after the second HTR at the same temperature. It should be pointed out that no significant  $O_2$  consumption was observed in the  $Nb_2O_5/SiO_2$  catalyst system after the same HTR treatment.

#### DISCUSSION

In  $Nb_2O_5$ -promoted Rh/ $SiO_2$  catalysts, the migration behaviors of Rh and  $Nb_2O_5$  particles depend on the calcination temperatures of the impregnated precursors on the silica surface. From the results obtained by X-ray diffraction (Fig. 1), the structure of the  $Nb_2O_5$ -promoted Rh/ $SiO_2$  catalysts calcined at different temperatures can be described by a model as shown in Fig. 7.

During calcination at 773 K, the precursors decompose to rhodium and niobium oxides. The  $Nb_2O_5$  is well dispersed, and most of the niobia particles may be located apart from  $Rh_2O_3$  particles on the silica surface (catalyst A). Most of such separated niobia particles are hardly reduced even by HTR treatment. Those  $Nb_2O_5$  promoter particles which are present in the vicinity of rhodium particles may be reduced in HTR

treatment. However, the amount is limited (0.1 in O/Rh value). The reduced niobia species block some of the surface Rh atoms to cause the decrease in  $H_2$  chemisorption capacity, but not sufficiently to induce strong Rh– $Nb_2O_5$  interaction, since no significant suppression was observed in the catalytic activity for the ethane hydrogenolysis reaction.

The particles of rhodium and niobium oxide are movable during calcination at higher temperatures. The calcination treatment at 973 K leads to a formation of three phases ( $Nb_2O_5$ ,  $Rh_2O_3$ , and  $RhNbO_4$ ) on the silica surface. During the calcination process, some of the  $Nb_2O_5$  particles migrate toward the  $Rh_2O_3$  particles and form a surface layer of  $RhNbO_4$  compound on them. The other  $Nb_2O_5$  particles agglomerated to larger ones (catalyst B) to form crystalline  $Nb_2O_5$ . In this catalyst, the significant SMSI effects (H/Rh diminished to zero and ethane hydrogenolysis activity suppressed by ca. 3.5 orders of magnitude) were observed after HTR treatment. The reduced niobia species may be formed from reduction of the  $RhNbO_4$  compound (32, 33). However, those  $Nb_2O_5$  particles which are located apart from the rhodium particles would not be reduced even by HTR treatment at 773 K. In practice, no reduction of  $Nb_2O_5$  oxide was observed by X-ray diffraction (Fig. 1, No. 3). The results indicate that the niobia species with its amount less than that of the total Rh atoms is sufficient to induce strong Rh– $Nb_2O_5$  interaction.

During high-temperature calcination at 1173 K, the larger particles of  $Nb_2O_5$  and  $Rh_2O_3$  are also movable. As a consequence of the reaction between rhodium and niobium oxide, almost a single phase of  $RhNbO_4$  was formed on the silica surface, accompanied by the disappearance of the  $Nb_2O_5$  and  $Rh_2O_3$  phases (catalyst C and catalyst B calcined at 1173 K). The high-temperature calcination caused significant sintering of particles, as indicated by the sharp diffraction peaks of the  $RhNbO_4$  compound.

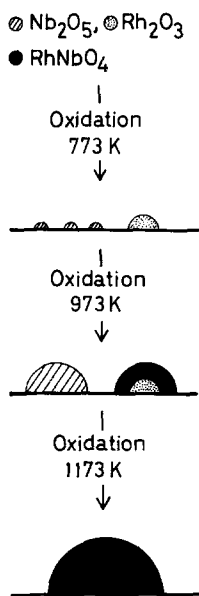
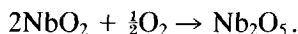


FIG. 7. Model for the formation of the  $RhNbO_4$  compound during the calcination process.

In catalyst C, the RhNbO<sub>4</sub> compound was formed almost exclusively on the silica surface. As indicated by the TPR spectra, the RhNbO<sub>4</sub> compound was reduced at much higher temperatures compared with Rh<sub>2</sub>O<sub>3</sub>. This compound can be reduced completely by HTR at 773 K. Significant SMSI effects were observed in this RhNbO<sub>4</sub>/SiO<sub>2</sub> catalyst. After HTR treatment at 773 K, the capacity of H<sub>2</sub> chemisorption diminished to zero, and the catalytic activity for ethane hydrogenolysis was suppressed by ca. 3.5 orders of magnitude compared with that after the following LTR treatment (39). From the comparison of catalyst A with catalyst B or C, severe suppression of catalytic activity for ethane hydrogenolysis was observed only after the H/Rh value diminished almost to zero (32). The results suggest that a nearly complete blockage of the Rh surface is required for a large SMSI effect.

This RhNbO<sub>4</sub>/SiO<sub>2</sub> catalyst system was used to characterize the Rh–Nb<sub>2</sub>O<sub>5</sub> interaction. After the first HTR treatment at 773 K, the NbO<sub>2</sub> phase was identified by X-ray diffraction (Fig. 4, Nos. 1 and 2). The results indicate clearly that NbO<sub>2</sub> is a reduction product of the RhNbO<sub>4</sub> compound. The amount of O<sub>2</sub> consumed by the oxidation of the reduced niobia species is 0.52 in O/Rh value after HTR treatment of the RhNbO<sub>4</sub>/SiO<sub>2</sub> catalyst at 773 K. This amount is in good agreement with 0.5 in O/Rh value which is predicted from the oxidation of NbO<sub>2</sub> to Nb<sub>2</sub>O<sub>5</sub>,



Therefore, the stoichiometry of the reduction of the RhNbO<sub>4</sub> compound by H<sub>2</sub> can be written as



The RhNbO<sub>4</sub> compound is reduced easily in comparison with Nb<sub>2</sub>O<sub>5</sub>. In catalyst B, no reduction of those Nb<sub>2</sub>O<sub>5</sub> particles was observed even after the same HTR treatment, as indicated by X-ray diffraction (Fig. 1, No. 3). Since significant SMSI ef-

fects were observed in this RhNbO<sub>4</sub>/SiO<sub>2</sub> catalyst after H<sub>2</sub> reduction at 773 K (HTR), the NbO<sub>2</sub> species thus formed should block surface Rh atoms to induce strong Rh–Nb<sub>2</sub>O<sub>5</sub> interaction.

The diffraction pattern of the Rh metal formed by HTR of catalyst C is also anomalous in comparison with the nonpromoted Rh/SiO<sub>2</sub> catalyst. Only the main peak of (111) line appeared in the XRD pattern, with almost no observed diffraction corresponding to (200) and (220) lines. For the nonpromoted Rh/SiO<sub>2</sub> catalyst, the intensities of (200) and (220) lines were about 40 and 30% of the (111) line (32). Thus, we can assume that the Rh particles formed by reduction of RhNbO<sub>4</sub> exist in a needle shape oriented mainly in the  $\langle 111 \rangle$  direction (38). The morphology change may be attributed to the strong interaction between rhodium and the niobia promoter.

After the RhNbO<sub>4</sub> compound was reduced, O<sub>2</sub> treatment at 773 K oxidized completely the reduced niobia species to Nb<sub>2</sub>O<sub>5</sub>. For the Rh particles, the surface layer is oxidized to Rh<sub>2</sub>O<sub>3</sub>, with the Rh core unchanged during this treatment. To obtain more precise information about the structure of this catalyst, the XRD pattern was recorded by a step-scan mode. As shown in Fig. 8, the diffraction lines of Rh<sub>2</sub>O<sub>3</sub> and Rh became clear. In addition, a small peak, which can be attributed to the most intensive diffraction of the RhNbO<sub>4</sub> phase, was also observed. It suggests that some surface precursor of RhNbO<sub>4</sub> can be formed, although the O<sub>2</sub> treatment at 773 K is not sufficient to induce the bulk reaction between rhodium and the niobia promoter. This result is also in agreement with that obtained from TPR studies.

After the second HTR treatment at 773 K, significant SMSI effects were also observed in H<sub>2</sub> chemisorption and the ethane hydrogenolysis reaction. As a part of the niobia promoter would be present in the vicinity of rhodium particles, the reduction of such niobium oxide may be catalyzed by the rhodium particles. Therefore, the re-

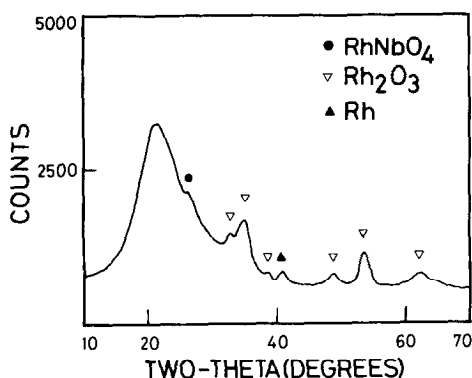


FIG. 8. X-ray diffraction pattern of catalyst C after being reduced in  $H_2$  at 773 K and calcined in  $O_2$  at 773 K. Step scan (step scan of  $0.04^\circ$ , present time of 20 s) was used.

duced niobia species can be formed from the reduction of the surface precursor of the  $RhNbO_4$  compound and some of the  $Nb_2O_5$  oxide in the vicinity of Rh particles. The formation of  $NbO_2$  species was also confirmed by X-ray diffraction (Fig. 4, No. 5). The amount is about 0.16 in O/Rh value according to the  $O_2$  consumption measurement. This value is significantly lower than that after the first HTR treatment. The result indicates again that the  $RhNbO_4$  compound is reduced easily in comparison with the  $Nb_2O_5$  particle, even though the reduction of a part of the latter can also be promoted by rhodium particles in the vicinity.

TPO measurements showed significant  $O_2$  consumption at the higher temperature side after  $H_2$  reduction either at 773 K or at 473 K (Fig. 6). However, the amount of  $O_2$  consumption at the lower temperature side changed greatly with the reduction temperature and procedure. The amount of this peak decreases in the following order: first HTR > second HTR >  $H_2$  reduction at 473 K. This trend is in good agreement with that obtained by the  $O_2$  consumption measurements in a vacuum system. As most of the rhodium oxide should be reduced after  $H_2$  reduction at 473 K, the excess amount of the  $O_2$  consumption at the lower temperature side should thus be attributed to the oxidation of the  $NbO_2$  species formed in the

HTR treatment. It should be pointed out that two maxima (453 and 540 K) were observed in the oxidation peak at the lower temperature side, suggesting that two kinds of  $NbO_2$  species exist in this  $Nb_2O_5$ -promoted Rh/ $SiO_2$  catalyst system after HTR treatment. We can speculate that  $O_2$  consumption around 453 K may be attributed to oxidation of the  $NbO_2$  species on the Rh particles, and that the peak around 540 K may be attributed to the reduced niobia species on the support. This subject will be discussed in our next paper (40).

The entire results given above can be rationalized by the model in Fig. 9 which represents the structure change of the  $RhNbO_4/SiO_2$  catalyst under thermal treatment in  $H_2$  or  $O_2$ , as follows.

As the catalyst was synthesized through high-temperature calcination, the  $RhNbO_4$  compound was well crystallized. The mean particle size is 139 Å according to the Scherrer formula of X-ray diffraction. The  $RhNbO_4$  compound cannot be reduced in  $H_2$  at temperatures lower than 473 K. After HTR treatment at 773 K, the  $RhNbO_4$  compound was reduced to Rh and  $NbO_2$ . At the

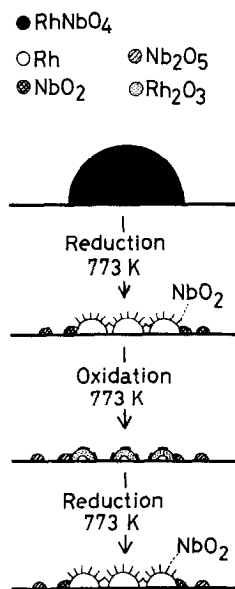


FIG. 9. Structure changes of the  $RhNbO_4$  particle during treatment in  $H_2$  or  $O_2$ .

same time, the large RhNbO<sub>4</sub> particle split into a number of smaller Rh particles. The mean size of the thus-formed Rh particles is 48 Å according to X-ray diffraction. During the following O<sub>2</sub> treatment at 773 K, NbO<sub>2</sub> is oxidized to Nb<sub>2</sub>O<sub>5</sub>. For the Rh particles, only the surface layer is oxidized to Rh<sub>2</sub>O<sub>3</sub>, with the Rh core remaining unchanged. Some surface precursor of the RhNbO<sub>4</sub> compound is also formed at the same time. After the second HTR treatment at 773 K, Rh<sub>2</sub>O<sub>3</sub> and the RhNbO<sub>4</sub> precursor is reduced to form Rh particles with surfaces covered with the NbO<sub>2</sub> species. Some of the Nb<sub>2</sub>O<sub>5</sub> promoter in the vicinity of Rh particles may also be reduced to NbO<sub>2</sub> during this treatment. For the two kinds of SMSI states of the Nb<sub>2</sub>O<sub>5</sub>-promoted Rh catalyst after the first and second HTR treatment (Fig. 9), the same extent of Rh-Nb<sub>2</sub>O<sub>5</sub> interaction was observed in the H<sub>2</sub> chemisorption and in the ethane hydrogenolysis reaction (39). However, the amount of the NbO<sub>2</sub> species is substantially different between the two states. This means that only a restricted amount of the reduced species, as suggested by the decoration model, is necessary for the strong Rh-Nb<sub>2</sub>O<sub>5</sub> interaction.

#### CONCLUSIONS

1. The single phase of the RhNbO<sub>4</sub> compound was formed on a silica surface through high-temperature calcination at 1173 K. This RhNbO<sub>4</sub> compound remained unchanged in H<sub>2</sub> at 473 K, but was reduced to Rh and NbO<sub>2</sub> during HTR treatment at 773 K.

2. The RhNbO<sub>4</sub>/SiO<sub>2</sub> catalyst, once it was decomposed by HTR treatment, exhibits significant SMSI behaviors: H<sub>2</sub> chemisorption capacity and activity of the ethane hydrogenolysis were suppressed severely by HTR and recovered after O<sub>2</sub> treatment at 673 K followed by LTR treatment.

3. NbO<sub>2</sub> species was formed in the Nb<sub>2</sub>O<sub>5</sub>-promoted Rh/SiO<sub>2</sub> catalyst after HTR treatment. It may be this NbO<sub>2</sub> spe-

cies which blocked the Rh surface, inducing the SMSI phenomena.

4. Rh redispersion occurred in the reduction process of the RhNbO<sub>4</sub> compound. The well-crystallized RhNbO<sub>4</sub> particle (139 Å) split into smaller Rh particles (48 Å) during HTR treatment.

#### ACKNOWLEDGMENTS

One of the authors (Z. Hu) thanks Tianjin University, China. This work was supported in part by a Grant-in-Aid for Scientific Research from the Ministry of Education, Science and Culture, Japan.

#### REFERENCES

1. Tauster, S. J., Fung, S. C., Baker, R. T. K., and Hounsely, J. A., *Science* **211**, 1121 (1981).
2. Haller, G. L., Henrich, V. E., McMillan, M., Resasco, D. E., Sadeghi, H. R., and Sakellson, S., in "Proceedings, 8th International Congress on Catalysis, Berlin, 1984," Vol. 5, p. 135. Dechema, Frankfurt-am-Main, 1984.
3. Van Den Berg, F. G. A., Glezer, J. H. E., and Sachtler, W. M. H., *J. Catal.* **93**, 340 (1985).
4. Lin, Y.-J., Resasco, D. E., and Haller, G. L., *J. Chem. Soc. Faraday Trans. 1* **83**, 2091 (1987).
5. Wilson, T. P., Kasai, P. H., and Ellg, P. C., *J. Catal.* **69**, 193 (1981).
6. Niemansverdriet, J. W., Van der Kraan, A. M., Van Loef, J. J., and Delgass, W. N., *J. Phys. Chem.* **87**, 1292 (1983).
7. Rieck, J. S., and Bell, A. T., *J. Catal.* **99**, 262 (1986).
8. Ichikawa, M., Fukushima, T., and Shikakura, K., in "Proceedings, 8th International Congress on Catalysis, Berlin, 1984," Vol. 2, p. 69. Dechema, Frankfurt-am-Main, 1984.
9. Vannice, M. A., *J. Catal.* **74**, 199 (1982).
10. Vannice, M. A., and Sudhaker, C., *J. Phys. Chem.* **88**, 2429 (1984).
11. Kunimori, K., Abe, H., Yamaguchi, E., Matsui, S., and Uchijima, T., in "Proceedings, 8th International Congress on Catalysis, Berlin, 1984," Vol. 5, p. 251. Dechema, Frankfurt-am-Main, 1984.
12. Singh, A. K., Pande, N. K., and Bell, A. T., *J. Catal.* **94**, 422 (1985).
13. Ko, E. I., Bafrali, R., Nuhfer, N. T., and Wanger, N. J., *J. Catal.* **95**, 260 (1985).
14. Kunimori, K., Doi, Y., Ito, K., and Uchijima, T., *J. Chem. Soc. Chem. Commun.*, 966 (1986).
15. Solymosi, F., *Catal. Rev.* **1**, 233 (1967).
16. Schwab, G. M., in "Advances in Catalysis" (D. D. Eley, P. W. Selwood, and Paul B. Weisz,

- Eds.), Vol. 27, p. 1. Academic Press, New York, 1978.
17. Tauster, S. J., Fung, S. C., and Garten, R. L., *J. Amer. Chem. Soc.* **100**, 170 (1978).
  18. Tauster, S. J., and Fung, S. C., *J. Catal.* **55**, 29 (1978).
  19. Santos, J., Phillips, J., and Dumesic, J. A., *J. Catal.* **81**, 147 (1983).
  20. Resasco, D. E., and Haller, G. L., *J. Catal.* **82**, 279 (1983).
  21. Sadeghi, H. R., and Henrich, V. E., *J. Catal.* **87**, 279 (1984).
  22. Belton, D. N., Sun, Y.-M., and White, J. M., *J. Phys. Chem.* **88**, 5172 (1984).
  23. Simoens, A. J., Baker, R. T. K., Dwyer, D. J., and Lund, C. R. F., and Madon, R. J., *J. Catal.* **86**, 359 (1984).
  24. Chung, Y.-W., Xiong, G., and Kao, C. C., *J. Catal.* **85**, 237 (1984).
  25. Takatani, S., and Chung, Y.-W., *J. Catal.* **90**, 75 (1984).
  26. Belton, D. N., Sun, Y.-M., and White, J. M., *J. Amer. Chem. Soc.* **106**, 3059 (1984).
  27. Ko, C. S., and Gorte, R. J., *J. Catal.* **90**, 59 (1984).
  28. Raupp, G. P., and Dumesic, J. A., *J. Catal.* **95**, 587 (1985).
  29. Mcviker, G. B., and Ziemiak, J. J., *J. Catal.* **95**, 473 (1985).
  30. Haller, G. L., and Resasco, D. E., to be published.
  31. Kip, B. J., Smeets, P. A. T., Van Wolput, J. H. M. C., Zandbergam, H. W., Van Grondelle, J., and Prins, R., *Appl. Catal.* **33**, 157 (1987).
  32. Hu, Z., Nakamura, H., Kunimori, K., Asano, H., and Uchijima, T., *J. Catal.* **112**, 478 (1988).
  33. Kunimori, K., Hu, Z., Ito, K., Maeda, A., Nakamura, H., and Uchijima, T., *Shokubai* [catalyst] **29**, 106 (1987); 59th CATSJ Meeting Abstracts, No. A16 (1987).
  34. Murakami, Y., in "Preparation of Catalyst" (G. Poncelet, P. Grange, and P. A. Jacobs, Eds.), p. 775. Elsevier, Amsterdam, 1983.
  35. Kunimori, K., Ikeda, Y., Soma, M., and Uchijima, T., *J. Catal.* **79**, 185 (1983).
  36. K. Kunimori, K. Ito, K. Iwai, and T. Uchijima, *Chem. Lett.*, 573 (1986).
  37. Shaplygin, I. S., Prosychev, I. I., and Lazarev, V. B., *Russ. J. Inorg. Chem. Eng. Transl.* **23**, 773 (1978).
  38. Yates, D. J. C., and Prestridge, E. B., *J. Catal.* **106**, 549 (1987).
  39. Hu, Z., Nakamura, H., Kunimori, K., and Uchijima, T., *Catal. Lett.* **1**, 271 (1988).
  40. Hu, Z., Kunimori, K., and Uchijima, T., to be published.